

Classification of initial state granularity via 2d Fourier expansion

C.E.Coleman-Smith,^{1,*} H.Petersen,¹ and R.L.Wolpert²

¹*Department of Physics, Duke University, Durham, NC 27708-0305*

²*Department of Statistical Science, Duke University, Durham, NC 27708-0251*

(Dated: December 3, 2024)

A new method to quantify fluctuations in the initial state of heavy ion collisions is presented. The initial state energy distribution is decomposed with a set of orthogonal basis functions which include both angular and radial variation. The resulting two dimensional Fourier coefficients provide additional information about the nature of the initial state fluctuations compared to a purely angular decomposition. We apply this method to ensembles of initial states generated by both Glauber and Color Glass Condensate Monte-Carlo codes. In addition initial state configurations with varying amounts of fluctuations generated by a dynamic transport approach are analysed to test the sensitivity of the procedure. The results allow for a full characterization of the initial state structures that is useful to discriminate the different initial state models currently in use.

Ultra-Relativistic nearly-ideal fluid dynamics has proven to be a very successful tool for modeling the bulk dynamics of the hot dense matter formed during a heavy ion collision [1–6]. The major uncertainty in determining transport properties of the QGP, such as the shear viscosity to entropy ratio, lies in the specification of the initial conditions of the collision. The initial conditions have been mainly assumed to be smooth distributions that are parametrized implementations of certain physical assumptions (e.g., Glauber/CGC). Within the last 2 years the importance of including fluctuations in these distributions has been recognized, leading to a whole new set of experimental observations of higher flow coefficients and their correlations [7–10]. On the theoretical side there has been a lot of effort to refine the previously schematic models with fluctuation inducing corrections and to employ dynamical descriptions of the early non-equilibrium evolution [11–14].

Hydrodynamical simulations can take these fluctuations into account by generating an ensemble of runs each with a unique initial condition, so-called *event by event* simulations. This is in contrast to *event averaged* simulations where an ensemble of fluctuating initial conditions is generated, and then a single initial condition corresponding to this set's ensemble average is subject to evolution. Event by event modeling has proven to be essential for correctly describing all the details of the bulk behavior of heavy ion collisions [15–25].

The two main models for the generation of hydrodynamic initial conditions are the Glauber [12, 26–28] and color glass condensate (CGC) models [29–34]. The Glauber model samples a Woods-Saxon nuclear density distribution for each nucleus.

Color glass condensate models are *ab initio* calculations motivated by the idea of gluon saturation of parton

distribution functions at small momentum scales x . In CGC models the gluon distribution for each nucleon is computed and the nuclear collision is modeled as interactions between these coherent color fields. Each of these models generates spatial fluctuations where the details depend on the assumptions used in the specific implementation. Glauber fluctuations come from Monte-Carlo (MC) sampling the nuclear density distribution. CGC fluctuations arise similarly with additional contributions from the self interaction of the color fields.

We present a method for generating a 2d decomposition of fluctuations in the initial state energy density of a heavy-ion collision. We apply this framework to the ensembles of initial states generated by UrQMD [35–37], by an MC Glauber code of Qin [12], and by the MC-KLN code of Drescher and Nara [29, 30, 38] which is a based on CGC ideas. The events compared are generated for Au+Au collisions at $\sqrt{s} = 200$ AGeV at two impact parameters $b = 2, 7$ fm. We introduce summary statistics for the Fourier expansion and show how the radial information exposes clear differences between the fluctuations generated by UrQMD and the MC-KLN codes.

Colliding nuclei are strongly Lorentz contracted along the beam axis, as such we neglect the longitudinal dimension. A priori we expect fluctuations in both radial and azimuthal directions. Experiments make measurements in a 2d momentum space, and further analysis of the final state may reveal correlations with quantities derived from a fully 2d decomposition of the initial state. Recent work by [39] has shown that events can be constructed which have identical ϵ_2, ϵ_3 but with dramatically different energy distributions leading to different final state flow coefficients. The structure of such events is not sensitive to an azimuthal only decomposition.

* cec24@phy.duke.edu

We seek a two dimensional Fourier expansion on a disk of radius r_0 . The orthogonality of Bessel functions of the first kind is the key to this decomposition

$$\int_0^{r_0} J_\alpha(r\lambda_{\alpha,n})J_\alpha(r\lambda_{\alpha,n'})rdr = \frac{r_0^2}{2}\delta_{nn'}[J_{\alpha+1}(\lambda_{\alpha,n})]^2, \quad \forall n, n' \in \mathbb{Z}, \forall \alpha \in \mathbb{R}, \quad (1)$$

where $\lambda_{\alpha,n}$ is the n^{th} positive zero of $J_\alpha(x)$. For integer α , $J_\alpha(-x) = (-1)^\alpha J_\alpha(x)$ and so $[J_{\alpha+1}(\lambda_{\alpha,n})]^2 = [J_{|\alpha|+1}(\lambda_{\alpha,n})]^2$, and $\lambda_{\alpha,n} = \lambda_{-\alpha,n}$. It follows that the functions

$$\phi_{m,n}(r, \theta) := \frac{1}{J_{|m|+1}(r_0\lambda_{m,n})} J_m(r\lambda_{m,n}) e^{im\theta} \quad (2)$$

form a complete orthonormal set on this disk (with the uniform measure $r dr d\theta / \pi r_0^2$). As such any well behaved function f on this disk admits the convergent expansion

$$f(r, \theta) = \sum_{m,n} A_{m,n} \phi_{m,n}(r, \theta), \quad (3)$$

in terms of these basis functions and a set of generalized Fourier coefficients $A_{m,n} \in \mathbb{C}$, defined as

$$A_{m,n} = \frac{1}{\pi r_0^2} \int f(r, \theta) \phi_{m,n}^*(r, \theta) r dr d\theta. \quad (4)$$

The basis functions $\phi_{m,n}$ are solutions to Bessel's equation on the unit disk [40]. They are the eigenfunctions of the Laplacian with Dirichlet bc and eigenvalue $-(\lambda_{m,n})^2$, such that

$$-\nabla^2 f(r, \theta) = \sum_{m,n} (\lambda_{m,n})^2 A_{m,n} \phi_{m,n}.$$

The eigenvalues of the Laplacian $\lambda_{m,n}^2$ define a characteristic inverse length scale for the associated Fourier component $A_{m,n}$. Higher orders of m and n are associated with larger $\lambda_{m,n}$ values corresponding to smaller spatial regions. A similar correspondence of length scales and 1d Fourier coefficients has been pointed out in [41, 42]. A selection of these eigenvalues are plotted in Fig: 1. Other boundary conditions (e.g., Neumann) lead to similar countable sets of basis functions.

Higher values of the angular indices $\pm m$ correspond to higher numbers of zero crossings in the angular components of basis functions, or ‘‘lumpiness’’ in rotation, while higher values of the radial indices n are associated with more roughness as one moves closer or farther from the center of mass. The first few basis functions are plotted in Fig: 2. The lumpy shape of the basis functions suggests that this representation will be very useful for characterizing the hot and cold spot structures in the initial state of a heavy ion reaction.

A typical UrQMD event (after subtraction of the ensemble average) is shown alongside its decomposition and

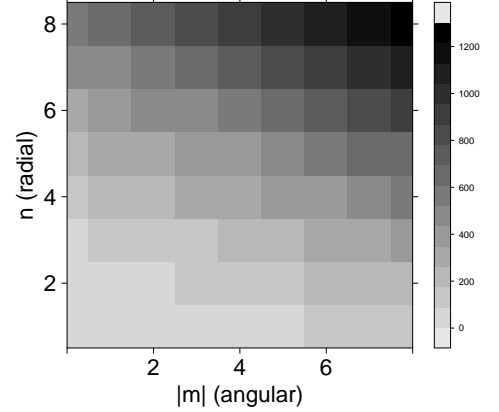


FIG. 1: The eigenvalues $\lambda_{m,n}^2$ of the negative Dirichlet Laplacian on the disk are plotted as a function of $|m|$ (angular) and n (radial). These can be interpreted as an inverse length scale for the coefficients $A_{m,n}$. Note that in general $|\lambda_{m+1,n} - \lambda_{m,n}| \neq |\lambda_{m,n+1} - \lambda_{m,n}|$, although $|\lambda_{m,n}| \asymp \pi(n + |m| - 1/4)$ as $n, m \rightarrow \infty$.

the resulting Fourier coefficients $A_{m,n}$ in Fig: 3. Here we characterize the event in terms of coefficients $m \in [-8, 8]$ and $n \in [1, 8]$, sufficient to capture a detailed image of the original initial state distribution. Higher order terms contribute very little additional information. The difference between the original distribution and the reconstructed distributions is dominated by numerical noise for coefficients with order higher than $m_{\text{max}} = 8, n_{\text{max}} = 8$. Let us now explore different ways to extract useful information from this decomposition.

Using the orthogonality of the basis functions along with the Laplacian we can derive simple expressions for norms of the function f to be expanded in the frequency domain. The $L_2(f)$ norm, which measures the total mass of f is,

$$L_2(f) := \langle f, f \rangle^{1/2} = \left[\sum |A_{m,n}|^2 \right]^{1/2}, \quad (5)$$

where $\langle a, b \rangle = \frac{1}{\pi r_0^2} \int_0^{r_0} a(r, \theta) b(r, \theta) r dr d\theta$ is the inner product for functions on our disk. The Sobolev $H_1(f)$ norm gives a measure of the total mass of the function as well as a measure of how ‘wobbly’ it is across the disk

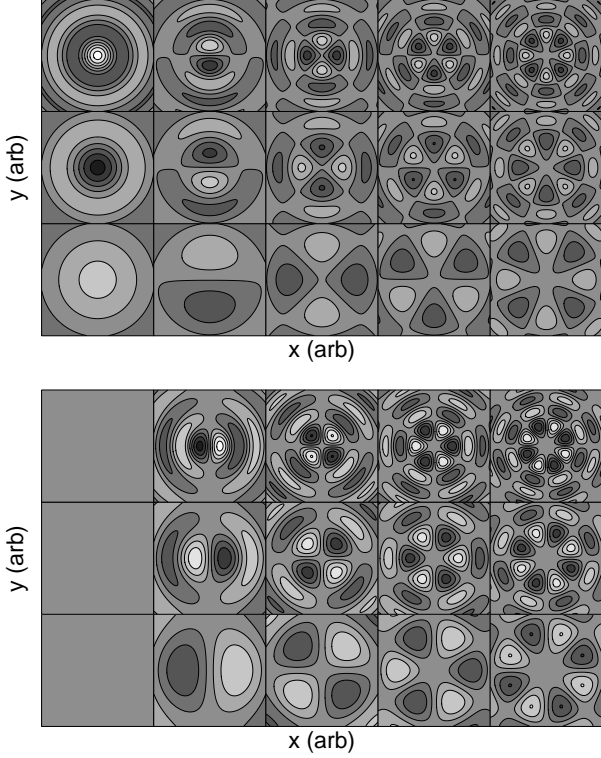


FIG. 2: Plots of the first few real (top) and imaginary (bottom) components of $\phi_{m,n}(r, \theta)$. The angular coefficient $m \in [0, 5]$ increases from left to right, the radial coefficient $n \in [1, 3]$ increases from bottom to top.

$$H_1(f) := \langle (-\ell^2 \nabla^2 + I)f, f \rangle^{1/2} = \left[\sum (\ell^2 \lambda_{m,n}^2 + 1) |A_{m,n}|^2 \right]^{1/2}, \quad (6)$$

where ℓ is a characteristic length scale introduced to maintain unit consistency (we use $\ell = 1$ fm). A variation on the Sobolev norm gives the angular norm $M_1(f)$ which quantifies angular gradients,

$$M_1(f) := \langle \partial_\theta^2 f, f \rangle^{1/2} = \left[\sum |m|^2 |A_{m,n}|^2 \right]^{1/2}. \quad (7)$$

We use these norms below to quantify properties of the events considered.

To demonstrate the usefulness of our proposed method, we apply it to three example models: UrQMD, MC-Glauber and MC-KLN. Since this work does not aim at drawing definitive conclusions about initial state physics these models should be regarded as representative of the models currently in use.

We consider a set of 100 events generated by each code. UrQMD includes Boltzmann hadronic transport before the hydro begins, while the MC-Glauber code includes simple streaming transport of the nucleons after interaction; both of these will introduce added spatial fluctuation in the energy density. The Glauber code also includes KNO scaling of the multiplicity fluctuations per

binary collision. For all models the initial condition was computed in a 200 point grid in the transverse plane at the center of the collision along the beam axis. To explore the centrality dependence of the analysis we consider events at two impact parameters $b = 2, 7$ fm. All events are generated for Au+Au collisions at $\sqrt{s_{NN}} = 200$ A GeV. To study the fluctuations generated by these events the ensemble averaged event is computed for each model and subtracted from each event in the ensemble before applying the decomposition.

In order to better understand the response of our process to fluctuations a series of progressively smoother ensembles of UrQMD events were generated. The degree of fluctuation is controlled by populating these ensembles with events created by averaging N independent events together. See [43] for more details on this process and its influence on the ellipticity and triangularity of the UrQMD initial state. As the number N of events over which we average increases, the result will increasingly resemble the ensemble average. We have examined events with $N = \{1, 2, 5, 10, 25\}$. While only the $N = 1$ case represents the true UrQMD output, the diminishing amounts of fluctuation in the other successively smoother sets can be used to give perspective on (or “calibrate”) our analysis.

In Fig:4 the ensemble averages of each norm (H_1 , M_1 , L_2) are plotted for each set of events. Considering first the UrQMD results it is clear that each norm tends to zero as N increases as expected, confirming that each norm is quantifying fluctuations. Fluctuations are lower at the larger impact parameter b but the relative ordering of the models is preserved. For all norms we see good agreement between the $N = 2$ UrQMD events and the MC-Glauber code.

The L_2 norm computes the total amount of fluctuation, the H_1 norm measures the spatial gradients in the fluctuations along with their total mass, the M_1 norm measures angular gradients. The MC-KLN results show the largest H_1 values while having M_1 values comparable to UrQMD $N = 1$, the MC-KLN L_2 is somewhat less than UrQMD. The relative ordering of the Glauber and UrQMD events is the same across all norms. The UrQMD and Glauber events are rather similar in the scale and nature of their fluctuations, UrQMD produces slightly larger fluctuations. The MC-KLN model produces fluctuations on a scale comparable to a hypothetical UrQMD $N = 3/2$. However the large H_1 and comparable M_1 implies that these events exhibit larger radial gradients than the other models. This may be attributed to the very rapid spatial falloff of the gluon density near the edges of the nucleons.

In Fig:5 we plot the ensemble distributions of the norms. The width of the UrQMD distributions shrinks with increasing N and the modes of the distributions shift towards smaller values. The averaging procedure reduces fluctuations, and the norms are sensitive to these fluctuations. Across the range of norms and impact parameters the MC-Glauber results follow the UrQMD $N = 2$ re-

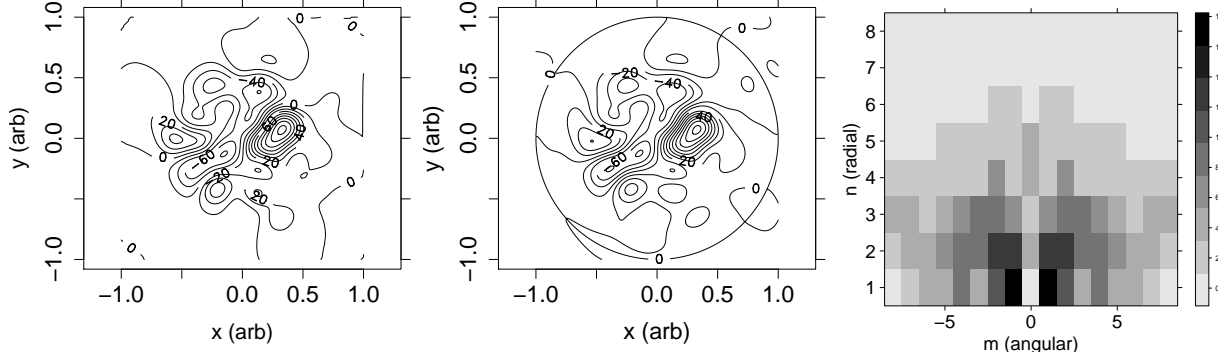


FIG. 3: A typical UrQMD ensemble average subtracted event. Second: the reconstructed event generated by (3) after applying the decomposition. Bottom: The absolute values of the Fourier coefficients $|A_{m,n}|$ for this event.

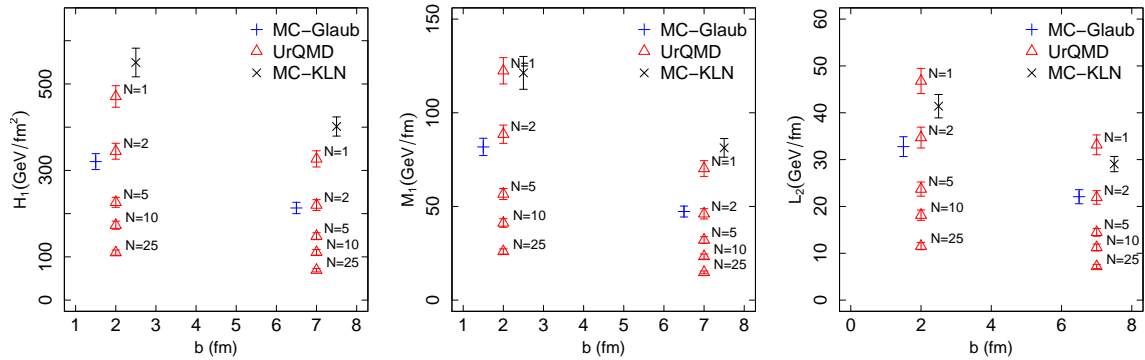


FIG. 4: The ensemble averages of the Sobolev norm H_1 (left) the angular norm M_1 (center) and the L_2 norm (right). The labels on the UrQMD glyphs give the number of averagings used to generate the ensemble members. The MC-Glauber and MC-KLN results are plotted with an artificial offset in b to permit easier comparison.

sults very closely. The MC-KLN code produces events with a larger range of H_1 values but with similar values to UrQMD N=1 for the other angular norm and slightly reduced total mass (L_2). The MC-KLN events show a wider range of spatial and angular gradients than the Glauber based models.

The ensemble average of the norms and their distributions are instructive summaries of the fluctuations produced by each model. In Fig:6 we show the ensemble averages of the absolute values of the Fourier coefficients $|A_{m,n}|$ plotted against their eigenvalues $\lambda_{m,n}$. These figures should be thought of as generalized power-spectra; states with higher coefficients contribute more to the fluctuations than those with lower weights. The figures are plotted with coefficients of constant n (radial degree) joined by lines. For all models we see that the Fourier weights decrease rapidly with increasing angular degree $|m|$, along the lines, and more slowly with increasing radial degree n at fixed m . These figures make it very clear that the different models produce quite different fluctuations.

It is informative to contrast the largest few coefficients for each model. As shown by the norms the UrQMD

and Glauber results are relatively similar—most of the weight is in coefficients with $n = 1, 2$ and $|m| = 0, 4$, corresponding to events with rather more angular variation and less radial variation. The bulk of the mass of the distributions is at $\lambda \sim 5 - 10$, implying that fluctuations with large length scales dominate.

The MC-KLN results stand in marked contrast. The largest weights are at $n = 2, 3, 4$ with $\lambda \approx 15$, representing basis states with more radial zero crossings and smaller characteristic sizes. We can conclude that the MC-KLN code generates fluctuations over smaller spatial scales with larger radial gradients compared to the Glauber based codes. These trends persist at both centralities, although the absolute scales are diminished at larger b . This is reasonable given that there is a smaller active collision area at higher impact parameters. The $2d$ Fourier decomposition is a straightforward method for capturing the differences in event structures in an intuitive way.

We have presented a new method for characterizing the fluctuations in the initial state of heavy ion collisions. The method is simple and general, it can be applied as easily to theoretical models as to the output of event gen-

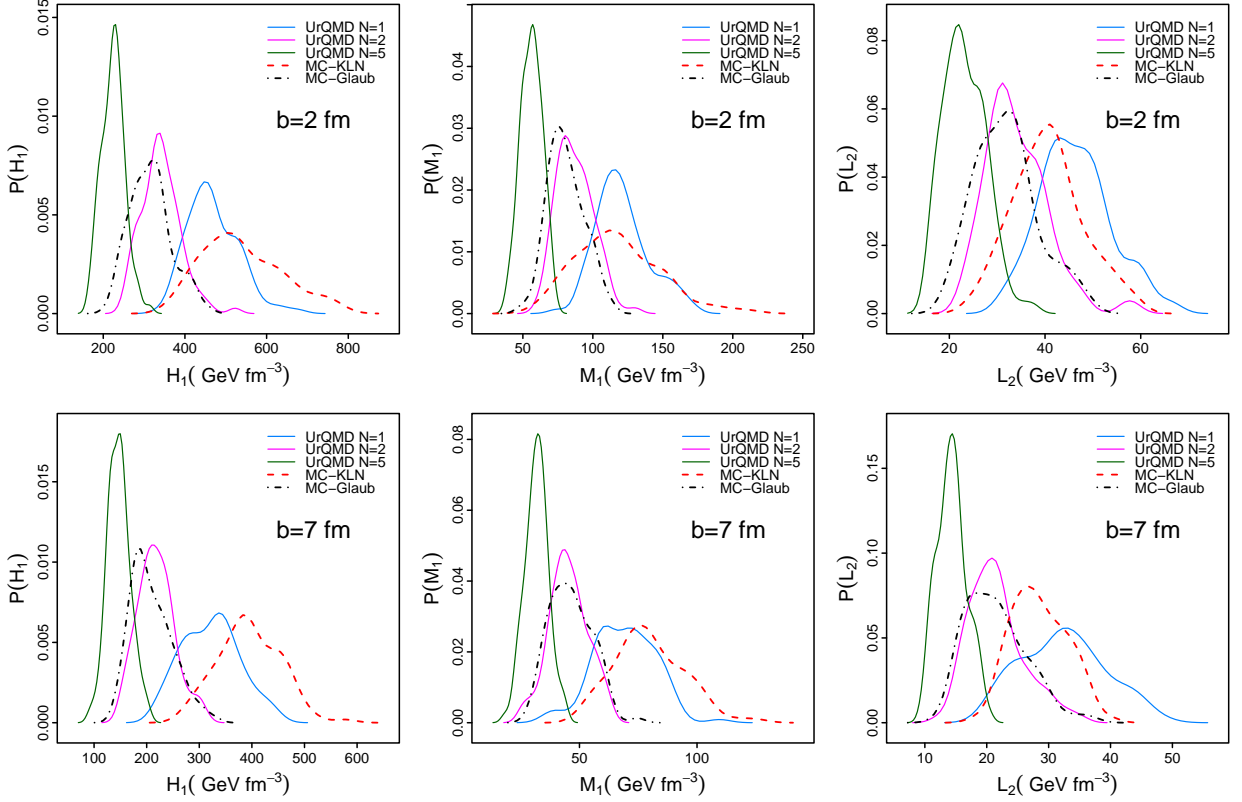


FIG. 5: The distribution of the H_1 (left), M_1 (middle) and L_2 (right) norms for UrQMD $N = \{1, 2, 5\}$, MC-KLN and MC-Glauber. The top row shows events at $b = 2$ fm, the bottom row shows $b = 7$ fm.

erators. We have shown the ability of the norms we introduce to quantify the broad differences among the three models we considered. The radial information included by this process provides additional insights into the nature of fluctuations which are not readily attainable by considering quantities derived from angular decompositions alone.

We believe that these quantities and variants will prove to be useful tools for further understanding the differences and similarities between initial condition models. They represent a reasonable compromise between too much information, as given by the full distributions of $|A_{m,n}|$ above, and too little information as given by event shape measures which marginalize away the radial information. In future work we will examine how these structures are passed through the hydrodynamical evolution to the hadronic final-state of the collision. Even if these quantities cannot be measured in detectors they provide a useful basis for apples-to-apples comparison of initial state models.

ACKNOWLEDGMENTS

The authors would like to thank G.Y. Qin for providing the MC-Glauber code. This work was supported by U.S.

Department of Energy grant DE-FG02-05ER41367 with computing resources from the OSG EngageVo funded by NSF award 075335, by NSF grants DMS-0757549 and PHY-0941373, and by NASA grant NNX09AK60G. Any opinions, findings, and conclusions or recommendations expressed in this material are those of the authors and do not necessarily reflect the views of the NSF or NASA.

Appendix: Angular Decomposition

To connect our analysis with commonly used quantities we quote in Table I the values of ϵ_2 and ϵ_3 computed for events without ensemble average subtraction.

	b (fm)	$E[\langle\epsilon_2\rangle]$	$E[\langle\epsilon_3\rangle]$
UrQMD, $N = 1$	2	0.096 ± 0.005	0.079 ± 0.004
MC-KLN	2	0.084 ± 0.005	0.046 ± 0.003
MC-GLAUB	2	0.089 ± 0.005	0.070 ± 0.004
UrQMD, $N = 1$	7	0.271 ± 0.010	0.117 ± 0.006
MC-KLN	7	0.343 ± 0.010	0.111 ± 0.006
MC-GLAUB	7	0.231 ± 0.009	0.099 ± 0.006

TABLE I: The ensemble average values of $\langle\epsilon_2\rangle$ and $\langle\epsilon_3\rangle$ for each of the models at impact parameters $b = 2, 7$ fm.

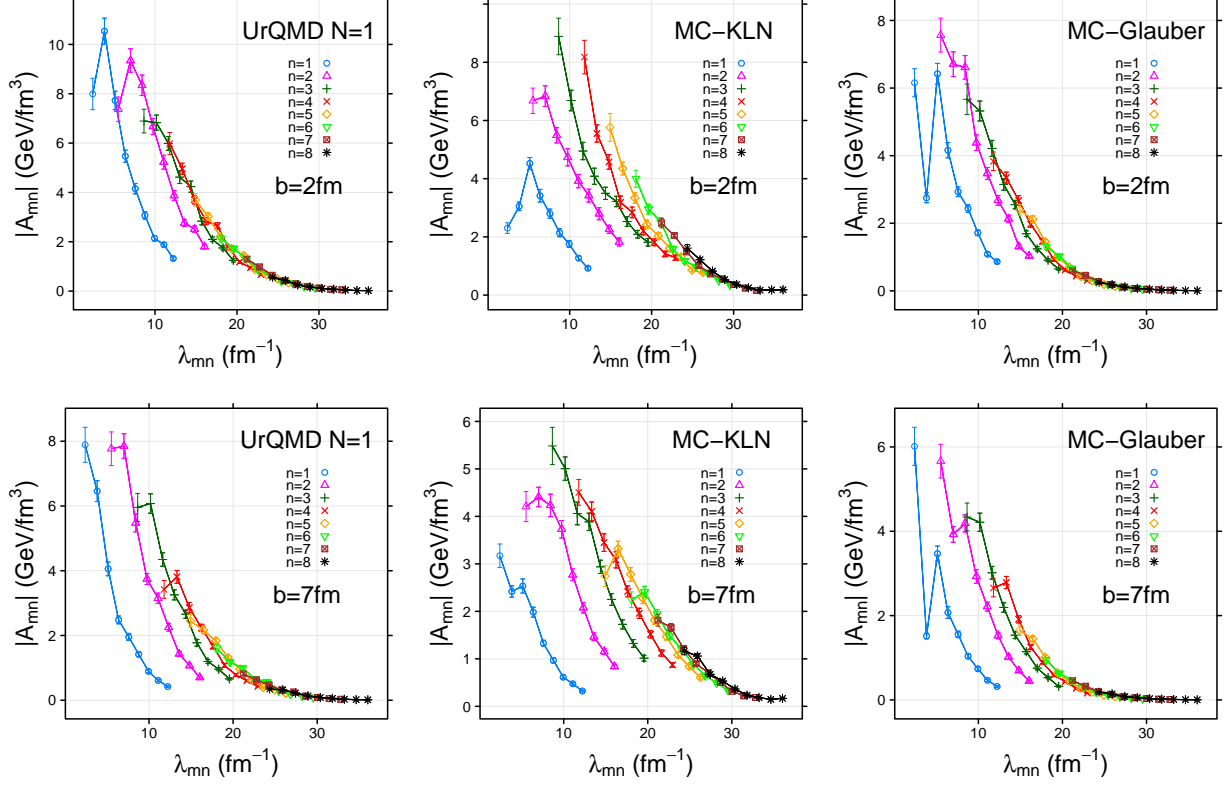


FIG. 6: Comparison of $|A_{m,n}|$ (points) plotted against the characteristic length eigenvalue $\lambda_{m,n}$ at $b = 2 \text{ fm}$ (top) and $b = 7 \text{ fm}$ (bottom). The solid lines join points with constant $n \in [1, 8]$ the angular components included are in the range $|m| \in [0, 8]$. For a given n value the $|m|$ distribution is monotonic, i.e., $|m| = 0$ is always the leftmost point on the line and $|m| = 8$ is always the rightmost.

-
- [1] H. Song, S. A. Bass, U. Heinz, T. Hirano, and C. Shen, *Phys.Rev.Lett.* **106**, 192301 (2011).
 - [2] C. Nonaka and S. A. Bass, *Phys.Rev.* **C75**, 014902 (2007).
 - [3] P. Huovinen, P. Kolb, U. W. Heinz, P. Ruuskanen, and S. Voloshin, *Phys.Lett.* **B503**, 58 (2001).
 - [4] B. Schenke, S. Jeon, and C. Gale, *Phys.Rev.* **C82**, 014903 (2010).
 - [5] P. Huovinen, *Nucl.Phys.* **A761**, 296 (2005).
 - [6] T. Hirano and K. Tsuda, *Phys.Rev.* **C66**, 054905 (2002).
 - [7] Z. Qiu, C. Shen, and U. Heinz, *Phys.Lett.* **B707**, 151 (2012).
 - [8] B. Schenke, S. Jeon, and C. Gale, *Phys.Rev.Lett.* **106**, 042301 (2011).
 - [9] B. H. Alver, C. Gombeaud, M. Luzum, and J.-Y. Ollitrault, *Phys.Rev.* **C82**, 034913 (2010).
 - [10] D. Teaney and L. Yan, *Phys.Rev.* **C83**, 064904 (2011).
 - [11] B. Schenke, P. Tribedy, and R. Venugopalan, (2012), arXiv:1202.6646 [nucl-th].
 - [12] G.-Y. Qin, H. Petersen, S. A. Bass, and B. Muller, *Phys.Rev.* **C82**, 064903 (2010).
 - [13] A. Dumitru and Y. Nara, *Phys.Rev.* **C85**, 034907 (2012).
 - [14] M. Alvioli, H. Holopainen, K. Eskola, and M. Strikman, *Phys.Rev.* **C85**, 034902 (2012).
 - [15] Z. Qiu and U. W. Heinz, *Phys.Rev.* **C84**, 024911 (2011).
 - [16] P. Staig and E. Shuryak, *Phys.Rev.* **C84**, 044912 (2011).
 - [17] M. Bleicher, L. Gerland, C. Spieles, A. Dumitru, S. Bass, *et al.*, *Nucl.Phys.* **A638**, 391 (1998).
 - [18] F. Grassi, Y. Hama, O. Socolowski, and T. Kodama, *J.Phys.G* **G31**, S1041 (2005).
 - [19] B. Tavares, H.-J. Drescher, and T. Kodama, *Braz.J.Phys.* **37**, 41 (2007).
 - [20] R. Andrade, F. Grassi, Y. Hama, T. Kodama, and J. Socolowski, O., *Phys.Rev.Lett.* **97**, 202302 (2006).
 - [21] R. Andrade, F. Grassi, Y. Hama, T. Kodama, and W. Qian, *Phys.Rev.Lett.* **101**, 112301 (2008).
 - [22] R. P. G. Andrade, F. Grassi, Y. Hama, and W.-L. Qian, (2010), 1008.4612.
 - [23] H. Holopainen, H. Niemi, and K. J. Eskola, *Phys.Rev.* **C83**, 034901 (2011).
 - [24] K. Werner, I. Karpenko, T. Pierog, M. Bleicher, and K. Mikhailov, *Phys.Rev.* **C82**, 044904 (2010).
 - [25] H. Petersen, G.-Y. Qin, S. A. Bass, and B. Muller, *Phys.Rev.* **C82**, 041901 (2010).
 - [26] R. Glauber and G. Mattaie, *Nucl.Phys.B* **B21**, 135 (1970).
 - [27] M. L. Miller, K. Reygers, S. J. Sanders, and P. Steinberg, *Ann.Rev.Nucl.Part.Sci.* **57**, 205 (2007).
 - [28] S. Esumi (PHENIX Collaboration), *J.Phys.G* **G38**, 124010 (2011), arXiv:1110.3223 [nucl-ex].
 - [29] D. Kharzeev and M. Nardi, *Phys Lett B* **B507**, 121 (2001).
 - [30] D. Kharzeev and E. Levin, *Phys Lett B* **B523**, 79 (2001).
 - [31] F. Gelis, E. Iancu, J. Jalilian-Marian, and R. Venugopalan, *Ann.Rev.Nucl.Part.Sci.* **60**, 463 (2010).
 - [32] A. Kovner, L. D. McLerran, and H. Weigert, *Phys.Rev.* **D52**, 3809 (1995).
 - [33] A. Krasnitz and R. Venugopalan, *Phys.Rev.Lett.* **84**, 4309 (2000).
 - [34] L. D. McLerran and R. Venugopalan, *Phys.Rev.* **D50**, 2225 (1994).
 - [35] S. Bass, M. Belkacem, M. Bleicher, M. Brandstetter, L. Bravina, *et al.*, *Prog.Part.Nucl.Phys.* **41**, 255 (1998).
 - [36] M. Bleicher, E. Zabrodin, C. Spieles, S. Bass, C. Ernst, *et al.*, *J.Phys.G* **G25**, 1859 (1999).
 - [37] H. Petersen, J. Steinheimer, G. Bureau, M. Bleicher, and H. Stocker, *Phys.Rev.* **C78**, 044901 (2008).
 - [38] H.-J. Drescher and Y. Nara, *Phys.Rev.* **C75**, 034905 (2007).
 - [39] F. G. Gardim, Y. Hama, and F. Grassi, (2011).
 - [40] M. Abramowitz and I. Stegun, *Handbook of Mathematical Functions* (Dover, New York, 1972).
 - [41] A. Mocsy and P. Sorensen, (2010), arXiv:1008.3381 [hep-ph].
 - [42] P. Staig and E. Shuryak, *Phys.Rev.* **C84**, 034908 (2011).
 - [43] H. Petersen, R. La Placa, and S. A. Bass, *J.Phys.G* **G39**, 055102 (2012).